Protonated Porphyrins: Bifunctional Catalysts for the Metal-Free Synthesis of *N*-Alkyl-Oxazolidinones

Matteo Cavalleri,[a] Caterina Damiano,[a] Gabriele Manca,*[b] and Emma Gallo*[a]

Abstract: The protonation of commercially available porphyrin ligands yields a class of bifunctional catalysts able to promote the synthesis of *N*-alkyl oxazolidinones by CO_2 cycloaddition to corresponding aziridines. The catalytic system does not require the presence of any Lewis base or additive, and shows interesting features both in terms of cost effectiveness and eco-compatibility. The metal-free method-ology is active even with a low catalytic loading of 1% mol, and the chemical stability of the protonated porphyrin allowed it to be recycled three times without any decrease in performance. In addition, a DFT study was performed in order to suggest how a simple protonated porphyrin can mediate CO_2 cycloaddition to aziridines to yield oxazolidinones.
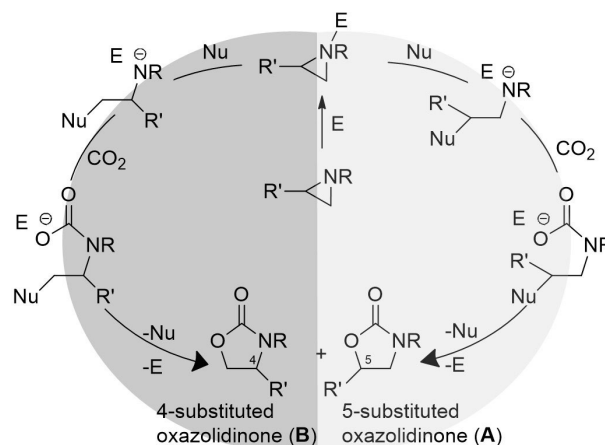
Introduction

The use of CO_2 as a C_1 source for synthesizing added-value compounds occupies a prominent role in the optimization of resource efficiency,[1–6] which is necessary for the transition from linear to circular chemical processes. One of the synthetic routes using carbon dioxide as a renewable reagent is its cycloaddition to three-membered rings such as epoxides[7–12] and aziridines. In particular, the reaction of the latter molecules with CO_2 is a 100% atom-economic procedure forming oxazolidinones,[13] which are largely employed as chiral auxiliaries[14] in organic synthesis as well as building blocks for producing pharmaceuticals.[15–18]

The synthesis of oxazolidinones is efficiently promoted by both homogeneous[19–21] and heterogeneous[22–25] catalytic systems, which are not always in line with dictates of green chemistry. In order to enhance catalytic performances, either high temperatures and CO_2 pressures or the presence of promoters, often obtained by nontrivial and time-consuming syntheses, are required. Consequently, the development of more eco-compatible protocols is an important goal and many efforts are currently devoted to apply catalytic systems which, besides being efficient and selective, can be recycled and reused several times.

Even if ammonium salts,[26,27] ionic liquids[28,29] N-heterocyclic olefins[30] can be used alone to promote the reaction of aziridines with CO_2, catalytic performances usually enhance in the presence of binary systems[28,30–34] constituted by an electrophilic (E) and nucleophilic (Nu) species, which play synergic roles in optimizing the catalytic efficiency as well as improving the reaction regioselectivity. As reported in Scheme 1, the reaction can form the two regioisomers **A** and **B** and the nature of the electrophilic species is fundamental to drive the nucleophilic attack to the aziridine ring and maximize the reaction regioselectivity.

Besides catalytic systems employed for promoting the synthesis of oxazolidinones by reacting aziridines with CO_2, porphyrin-based catalytic procedures[35–38] demonstrated to be very efficient and selective. The activity of ruthenium porphyrin

[a] M. Cavalleri, Dr. C. Damiano, Prof. E. Gallo
Department of Chemistry, University of Milan
Via C. Golgi 19, 20133 Milan (Italy)
E-mail: emma.gallo@unimi.it

[b] Dr. Dr. G. Manca
Istituto di Chimica dei Composti OrganoMetallici
ICCOM-CNR
Via Madonna del Piano 10, 50019 Sesto Fiorentino (Italy)
E-mail: gabriele.manca@iccom.cnr.it

Scheme 1. General scheme of the synthesis of the two oxazolidinone regioisomers.

Chemistry–A European Journal

Research Article
doi.org/10.1002/chem.202202729

Chemistry
Europe
European Chemical
Societies Publishing

complexes[39] was first investigated by some of us and more recently we also discovered the capability of metal-free porphyrins in mediating the synthesis of *N*-substituted oxazolidinones.[40–42]

Considering that TPPH$_2$ (TPP = dianion of tetraphenyl porphyrin) was very active in the presence of TBACl (tetrabutylammonium chloride), which furnish the chloride nucleophilic anion in charge of the ring-opening process, we wondered if a chlorohydrate porphyrin was able to play a bifunctional role by furnishing both the porphyrin platform to induce the regioselectivity and the Cl⁻ anion to attack the aziridine ring.

On the basis of this hypothesis, we investigated the activity of simple and low-cost protonated porphyrins with the low catalytic loading of 1 mol% and in the absence of any additive or Lewis base. Collected data are here reported alongside the DFT investigation of the reaction mechanism.
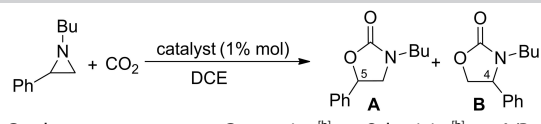
Results and Discussion

Synthetic study

The protonated porphyrins shown in Scheme 2 were synthesized by adding either an aqueous solution of HX[43] or RCOOH[44] to a dichloromethane solution of TPPH$_2$.

Porphyrins TPPH$_4$X$_2$ (**1**, X = Cl; **2**, X = Br; **3**, X = I) and TPPH$_4$(RCOO)$_2$ (**4**, R = CF$_3$; **5**, R = ClCH$_2$; **6**, R = Cl$_2$CH) were obtained in a quantitative yield, fully characterized (see the Supporting Information) and tested in the synthesis of *N*-butyl-phenyloxazolidin-2-one (**7**; Table 1).
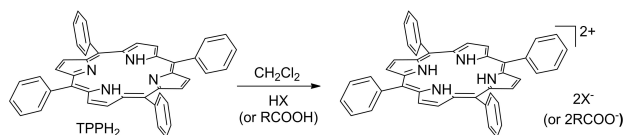
Scheme 2. Synthesis of protonated porphyrins **1–6**.

Table 1. Synthesis of *N*-butyl-phenyloxazolidin-2-one (**7**) promoted by porphyrins **1–6**.[a]

	Catalyst	Conversion[b]	Selectivity[b]	A/B ratio[b]
1	TPPH$_4$Cl$_2$ (**1**)	60	100	95:5
2	TPPH$_4$Br$_2$ (**2**)	84	88	95:5
3	TPPH$_4$I$_2$ (**3**)	100	54	95:5
4	TPPH$_4$(CF$_3$COO)$_2$ (**4**)	8	100	95:5
5	TPPH$_4$(ClCH$_2$COO)$_2$ (**5**)	27	100	95:5
6	TPPH$_4$(Cl$_2$CHCOO)$_2$ (**6**)	8	100	95:5
7	HCl (37% aq)[c]	39	95	90:10

[a] Reaction mixtures were stirred at 100 °C for 6 h in 0.5 mL of dichloroethane (DCE) with 1% of catalyst (8×10⁻⁶ mol) under 1.2 MPa of CO$_2$ pressure. [b] Calculated by ¹H NMR spectroscopy by using 2,4-dinitrotoluene as the internal standard. [c] 2% mol.

The model reaction shown in Table 1 was run for only 6 h to better compare the catalytic efficiency of tested catalysts. As reported, all the catalytic reactions showed the same regioselectivity independently from the nature and nucleophilicity of the anion. On the other hand, considering that cycloaddition reactions occur without producing by-products, the 100% of selectivity, which was observed in the presence of catalysts **1**, **4**, **5** and **6** (Table 1, entries 1 and 4–6), can be an interesting starting point to maximize the reaction sustainability by also avoiding the formation of side products.

In order to choose the best catalyst for studying the reaction scope, we investigated the chemical stability of complexes **1–6** by treating them at 100 °C in dichloroethane (DCE) under 1.2 MPa of CO$_2$ for 16 h and in the absence of *N*-butyl-2-phenylaziridine. The ¹H NMR analysis of all the tested reaction mixtures performed after 16 h revealed a similar stability for all the catalysts **1–6**. The presence of neither free-base (neutral) porphyrins nor decomposition products was detected.
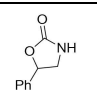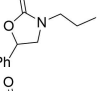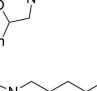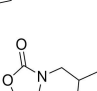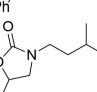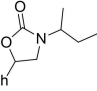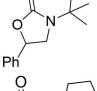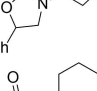
Even if all the tested catalysts were equally stable, in view of the importance to develop low-cost catalytic systems, TPPH$_4$Cl$_2$ (**1**) was chosen as the target catalyst alongside TPPH$_4$Br$_2$ (**2**), which also showed a good conversion/selectivity relationship (Table 1). Although it is worth investigating the catalytic activity of both complexes, TPPH$_4$Cl$_2$ (**1**) has to be considered more convenient than TPPH$_4$Br$_2$ (**2**) due to the lower cost, toxicity and the corrosive nature of HCl with respect to HBr. In addition, the 100% selectivity observed in the presence of catalyst **1** ensures the absence of any side products, whose presence decreases the reaction sustainability.

Thus, the experimental conditions of the model reaction catalyzed by TPPH$_4$Cl$_2$ (**1**) were optimized by testing different solvents, reaction temperatures, reaction times, CO$_2$ pressures and catalytic loading. The resulting data, reported in the Supporting Information, indicated good performance by running the reaction for 16 h at 100 °C with 1.2 MPa of CO$_2$ and 1% mol of catalytic loading.
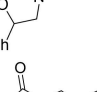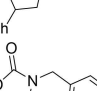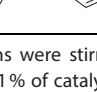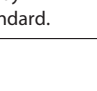
The experimental conditions described above were employed to study the reaction scope in the presence of TPPH$_4$Cl$_2$ (**1**) and achieved data were compared to those collected by running the reactions in the presence of TPPH$_4$Br$_2$ (**2**). Except in two cases (Table 2, entries 2 and 3), the regioisomer **A** was always formed as the sole product to testify the high regioselectivity of the catalytic system; collected results are listed in Table 2. Apart from the synthesis of compound **8** (entry 1), where the moderate yield can be due to chemical instability of the starting aziridine with respect to all the other reagents, the length of linear alkyl substituents did not affect the performance of the reaction (entries 2–4). Conversely, achieved data indicated the negative influence of the steric hindrance of the branched substituent at the aziridine nitrogen atom on the catalytic performance and a drastic decrease of the reaction productivity was observed when the nitrogen atom beard a *sec*-butyl and a *tert*-butyl substituent; only traces of compounds **13** and **14** were formed (entries 5–8).

The presence of N-cyclic substituents did not allow the formation of oxazolidinones **15** and **16** in good yields both

Chemistry–A European Journal

Research Article
doi.org/10.1002/chem.202202729

Chemistry Europe
European Chemical
Societies Publishing

Table 2. Study of the reaction scope in the presence of catalysts TPPH$_4$Cl$_2$ (**1**) and TPPH$_4$Br$_2$ (**2**).[a]

	Product		Catalyst **1**		Catalyst **2**	
			Yield [%][b]	A/B ratio[b]	Yield [%][b]	A/B ratio[b]
1		**8**	71	100:0	71	100:0
2		**9**	100	95:5	100	95:5
3		**7**	100	95:5	100	95:5
4		**10**	100	100:0	100	100:0
5		**11**	69	100:0	100	100:0
6		**12**	100	100:0	100	100:0
7		**13**	traces	–	traces	–
8		**14**	traces	–	traces	–
9		**15**	20	100:0	30	100:0
10		**16**	23	100:0	30	100:0
11		**17**	100	100:0	65	100:0
12		**18**	61	100:0	100	100:0

[a] Reactions were stirred at 100 °C for 16 h in 0.5 mL of dichloroethane (DCE) with 1% of catalyst (8×10^{-6} mol) under 1.2 MPa of CO$_2$ pressure. [b] Calculated by ^{1}H NMR spectroscopy by using 2,4-dinitrotoluene as the internal standard.

run in the presence of 2% mol of HCl (37% in water; see the Supporting Information for experimental details). The desired compound was formed with 39% of aziridine conversion and 95% of selectivity (37% yield) with an **A/B** ratio of 90:10 (Table 1, entries 7) confirming the active catalytic role of chlorohydrate porphyrin.
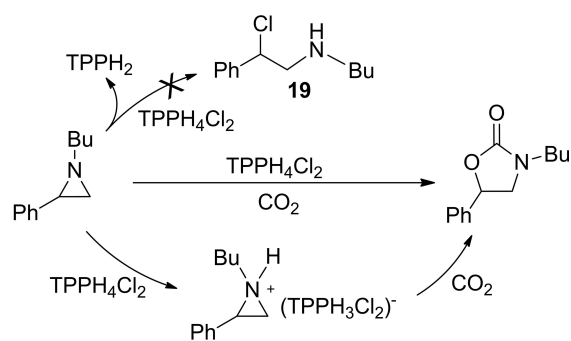
In addition, the chemical stability of **1** was further investigated by repeating the synthesis of oxazolidinone **7** for three consecutive times. All the reactions, performed by using the optimized experimental conditions reported in Table 2, occurred with a complete aziridine conversion and compound **7** was formed with a 100% of selectivity and **A/B** ratio of 95:5. The positive recycle test confirmed the high chemical robustness of TPPH$_4$Cl$_2$ (**1**) that guarantees a good sustainability of the process and paves the way for an implementation of the system.

In view of the general convenience in using **1** rather than **2**, the first was employed to study the reaction mechanism, whose comprehension could be useful to enhance the catalytic efficiency of the catalytic system.

Mechanistic study

The reactivity of catalyst **1** with respect to the two reagents (CO$_2$ and aziridine) was first analyzed. While no reaction was observed by treating **1** under 1.2 MPa of CO$_2$ at 100 °C, a modification of ^{1}H NMR aziridine aromatic signals was observed by adding **1** to the THF solution of N-butyl-2-phenylaziridine. Spectra reported in the Supporting Information suggested an interaction between TPPH$_4$Cl$_2$ (**1**) and aziridine that can be due either to the formation of hydrogen bonding between H atoms of the porphyrin core and the basic N atom of the aziridine ring or a ring-opening reaction[45] yielding β-chloroamine **19** (Scheme 3).

In order to better clarify the nature of this interaction, **19** was otherwise synthesized and characterized (see the Supporting Information for experimental details). Its ^{1}H NMR spectrum was compared to that obtained by treating N-butyl-2-phenyl-aziridine with **1** at 100 °C in both THF and DCE which, presenting a different polarity, can differently assist the aziridine protonation. In view of the non-similarity between NMR spectra,

using catalyst **1** or **2** (entries 9 and 10). While catalyst **1** was more performant in the synthesis of **17** (entry 11), catalyst **2** was more active than **1** in mediating the synthesis of **18** (entry 12). As reported, the regioselectivity of the formation of compounds **15–18** was always complete towards the formation of **A**, independently from the nature of the nitrogen substituent. Unfortunately, both catalysts did not promote the synthesis of N-aryl oxazolidinones.

In order to validate the catalytic efficiency of protonated porphyrins, the model reaction yielding oxazolidinone **7** was

Scheme 3. Possible involvement of β-chloroamine **19** as a catalytic intermediate.

we suggest that **19** was not formed under the employed experimental conditions and instead a simple protonation of the aziridine ring may occur (Scheme 3).

To definitely rule out the possible involvement of β-chloroamine species in the catalytic reaction, **19** was treated with 1.2 MPa of CO_2 in the presence of either TPPH$_4$Cl$_2$ (**1**) or TPPH$_2$. In both cases compound **19** was recovered unreacted indicating that it is not formed during the catalytic cycle, as also supported by the DFT study described in the following.

DFT study

Our previous studies on the formation of oxazolidin-2-ones mediated by TPPH$_2$/TBACl system revealed that the catalytic active species is an adduct between these species held together by very weak dispersion forces. This positive interaction renders Cl$^-$ anion nucleophilic enough toward the three-membered ring to drive the formation of the desired oxazolidinone.

As reported above, the replacement of TBACl by HCl resulted productive towards the oxazolidinone formation to suggest that also in this case the Cl$^-$ anion is active in promoting ring-opening reaction. The formation of TPPH$_4$Cl$_2$ (**1**) was studied by DFT calculations both in DCE and THF, the two solvents experimentally employed, and collected data revealed similar energy requirements. The reaction was exergonic with a free energy gain of -32.1 or -31.5 kcal mol^{-1} when calculations were performed in DCE or THF, respectively. The modelling of TPPH$_4$Cl$_2$ (**1**; Figure 1) revealed the formation of four *quasi*-equivalent H···Cl distances.

In order to formulate a mechanistic proposal for the TPPH$_4$Cl$_2$-catalyzed synthesis of oxazolidinones, three different possible reaction pathways were taken into account: a) activation of CO_2 followed by the interaction with the *N*-butyl-2-phenylaziridine; b) activation of *N*-butyl-2-phenylaziridine followed by the interaction with CO_2 and c) simultaneous activation of CO_2 and *N*-butyl-2-phenylaziridine.

a) Activation of CO_2 followed by the interaction with N-butyl-2-phenylaziridine

All efforts to localize interactions between the CO_2 oxygen atoms and the protons at the pyrrolic nitrogen atoms of **1** failed and the distance between these two species was always more than 3.0 Å to exclude the carbon dioxide activation. Considering
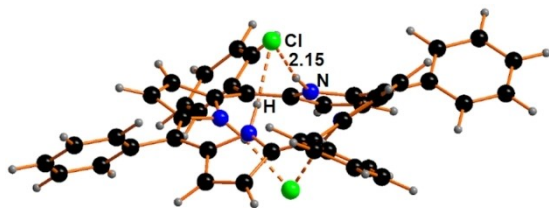
that identical results were obtained in DCE and in THF, this pathway was dismissed.

b) Activation of N-butyl-2-phenylaziridine followed by the interaction with CO_2

The DFT study revealed that the initial protonation of the aziridine nitrogen atom by **1** (Scheme 3) can be followed by the nucleophilic attack of the chloride anion to the aziridine ring forming the **1**/β-chloroamine adduct through ring-opening process. The energy profile of the process (see the Supporting Information for details), revealed that **1**/β-chloroamine adduct is less stable by 9.2 kcal mol^{-1} than **1**/*N*-butyl-2-phenylaziridine one indicating a probable reversibility of the reaction. Even if **1**/β-chloroamine adduct can be formed under employed experimental conditions (high temperatures), it should be immediately reconverted into **1**/*N*-butyl-2-phenylaziridine starting material.

In view of the experimental and computational results, the formation of **1**/β-chloroamine intermediate was discarded also in view of high free-energy barrier (higher than 32.0 kcal mol^{-1}), which is required for the transformation of β-chloroamine **19** into **7**. Such a result is in line with the unfavorable interaction between the low nucleophilic amino nitrogen atom of **19** and the incoming CO_2.

c) Combined activation of CO_2 and N-butyl-2-phenylaziridine

Once the stepwise activation of CO_2 and aziridine was dismissed, the combined activation of the two reagents was taken into account, as already proposed for the simultaneous activation of indole and CO_2 by bicyclic guanidine catalyst.[46] In particular, compound **20** was optimized and it shows CO_2 placed in between TPPH$_4$Cl$_2$ (**1**) and *N*-butyl-2-phenylaziridine. As shown in Figure 2, the oxygen of carbon dioxide interacts with the porphyrin NH moieties (O···H distance of 1.76 Å) and the formation of a linkage between the N$_{az}$ and the C3 atom of CO_2 occurs. In addition, CO_2 loses its linearity, as revealed by the O—C3—O angle of 134° and the presence of the active IR

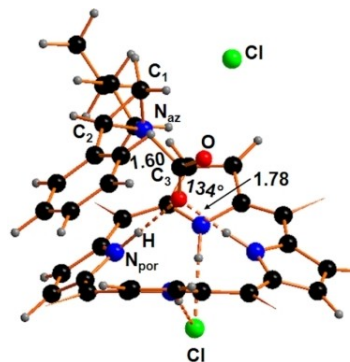**Figure 1.** Optimized structure of TPPH$_4$Cl$_2$ (**1**).

Figure 2. Optimized structure of **20**. The aromatic rings at the *meso* positions are omitted for clarity.

vibration at 1800 cm^{-1} (associated with the C—O stretching mode). The endergonic formation of **20** by $+18.8$ kcal mol^{-1} is mainly due to the disfavoring entropic term ($T\Delta S$) of $+24.8$ kcal mol^{-1} that negatively balances the favorable enthalpic term of -6.0 kcal mol^{-1}.

At this point, the chloride anion is able to perform the nucleophilic attack at the C1 atom with the formation of transition state **21$_{TS}$** (Figure 3a) with an associated low free energy barrier of $+1.5$ kcal mol^{-1}. Thus, the overall free energy barrier for the achievement of **21$_{TS}$** was calculated to be 20.3 kcal mol^{-1}. In order to achieve a more accurate value of this barrier, the solvation energy of the different involved species should be considered by using an explicit solvent model.[48,49] In that case, the expected free-energy barrier associated with **21$_{TS}$** should be higher than the calculated one and more in line with the employed experimental conditions. However, the high number of atoms to be modelled renders calculations very time-consuming and the correction was not introduced.

The formation of **21** (Figure 3b) is associated with a free energy gain of -11.1 kcal mol^{-1}.

The oxygen atom of **21** acquired a sufficient nucleophilic character to perform the ring-closing step forming *N*-butyl-phenyloxazolidin-2-one (**7**) and restoring catalyst **1**. DFT calculations allowed the transition state **7$_{TS}$** to be isolated (Figure 4) with an associated free energy barrier of $+8.9$ kcal mol^{-1}. The structure shows a quasi-linear O—C1—Cl alignment with an angle of 164°, a O—C1 distance of 2.32 Å and a C1—Cl bond elongated by about 0.3 Å. The environment around the C1 center becomes quasi-planar with a total angle sum of 352.1°, as occurs in a classic S$_N$2 reaction mechanism. After the formation
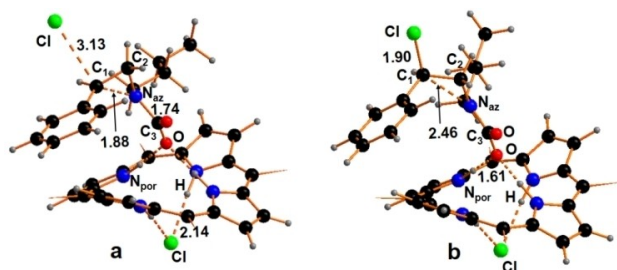
of **7$_{TS}$**, *N*-butyl-phenyloxazolidin-2-one (**7**) is formed with a free-energy gain of -22.8 kcal mol^{-1}, alongside catalyst **1**.

Summarizing, the overall free energy pathway of the formation of oxazolidinone **7** catalyzed by **1** occurs with a final free energy gain of -4.7 kcal mol^{-1}. The energy profile of the reaction is shown in Figure 5.

Conclusion

The protocol for synthesizing *N*-alkyl oxazolidinones reported here represents a very convenient methodology in view of the high sustainability of the catalytic system. Metal-free protonated porphyrins were easily synthesized by treating commercially available free-base porphyrins with mineral or organic acids. The bifunctional catalysts TPPH$_4$X$_2$ (X = Cl or Br) were active in the metal-free synthesis of several *N*-alkyl oxazolidinones even with a low catalytic loading of 1% mol. No Lewis base or additive was required. In addition, the very high chemical stability of TPPH$_4$Cl$_2$ allowed three consecutive reactions to be performed without any observable decrease in catalytic performance. A DFT study of the reaction mechanism revealed that the porphyrin protonation is a highly exergonic process and that the resulting catalyst promotes the synthesis of the desired oxazolidinone by a synergic activation of both of the reaction components (aziridine and CO$_2$). The applied TPPH$_4$X$_2$ catalyst furnishes both a porphyrin platform to induce good regioselectivity (up to 100%) and an active nucleophilic chloride anion for performing the ring-opening reaction.

In conclusion, the use of very cheap and eco-compatible TPPH$_4$X$_2$ catalysts for the CO$_2$ enhancement is in line with the society's request for the transformation of waste into resources by applying sustainable chemical processes. The ease of synthesizing catalysts and isolating the desired compounds in high yield, with high regioselectivities, and in the absence of stoichiometric by-products, confer a general low-cost applicability on the report methodology.

Figure 3. Optimized structures of a) **21$_{TS}$** and b) **21**. The aromatic rings at the *meso* positions are omitted for clarity.
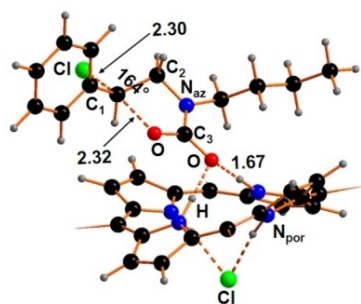

Figure 4. Optimized structure of transition state **7$_{TS}$**. The aromatic rings at the *meso* positions are omitted for clarity.
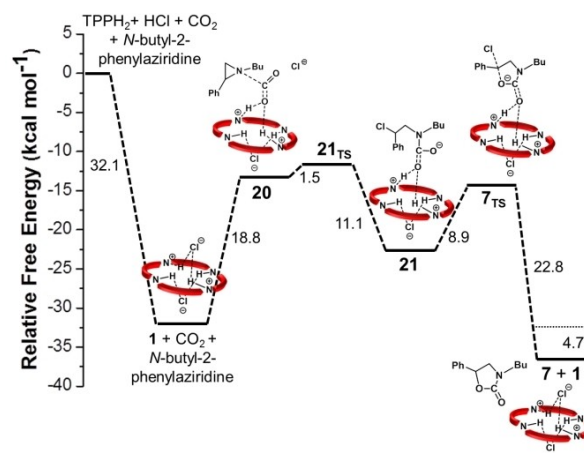

Figure 5. Free energy [kcal mol^{-1}] of the synthesis of **7**.

Experimental Section

General catalytic procedure: In a 3.5 mL glass liner equipped with a screw cap and glass wool, the desired catalyst (8×10^{-6} mol) and aziridine (8×10^{-4} mol) were dissolved in DCE (0.5 mL). The vessel was transferred into a stainless-steel autoclave and the required CO_2 pressure was charged at room temperature. The autoclave was placed in a preheated oil bath at the desired temperature, stirred for the required time and then quenched in an ice bath and slowly vented (see Tables 1 and 2 for experimental details). The solvent was evaporated to dryness and the crude analyzed by ^1H NMR spectroscopy by using 2,4-dinitrotoluene as the internal standard.

Computational details: The minima and transition states along the reaction pathway were isolated and characterized at B97D-DFT level of theory[47] within Gaussian 16 package.[50] All the optimized structures were validated as minima or transition states by the vibrational frequencies calculations. All the calculations were carried out within the CPCM model[51–52] for the tetrahydrofuran and dichloroethane, the experimentally used solvents. The 6-31G basis set, with the addition of the polarization functions (d, p) was adopted. The coordinates of all the optimized structures as well as their main energetic features are reported in the Supporting Information.

Conflict of Interest

The authors declare no conflict of interest.

Data Availability Statement

The data that support the findings of this study are available from the corresponding author upon reasonable request.

[1] A. Modak, P. Bhanja, S. Dutta, B. Chowdhury, A. Bhaumik, *Green Chem.* **2020**, *22*, 4002–4033.

[2] C. C. Truong, D. K. Mishra, *Environ. Chem. Lett.* **2020**, *19*, 911–940.

[3] M. N. Anwar, A. Fayyaz, N. F. Sohail, M. F. Khokhar, M. Baqar, A. Yasar, K. Rasool, A. Nazir, M. U. F. Raja, M. Rehan, M. Aghbashlo, M. Tabatabaei, A. S. Nizami, *J. Enenviron. Manag.* **2020**, *260*, 110059.

[4] Y. Yang, J.-W. Lee, *Chem. Sci.* **2019**, *10*, 3905–3926.

[5] J. Artz, T. E. Müller, K. Thenert, J. Kleinekorte, R. Meys, A. Sternberg, A. Bardow, W. Leitner, *Chem. Rev.* **2018**, *118*, 434–504.

[6] J. Zhang, C. D. Sewell, H. Huang, Z. Lin, *Adv. Energy Mater.* **2021**, *11*, 2102767.

[7] C. Claver, M. B. Yeamin, M. Reguero, A. M. Masdeu-Bultó, *Green Chem.* **2020**, *22*, 7665–7706.

[8] S. Kernbichl, B. Rieger, in *Engineering Solutions for CO_2 Conversion* (Eds.: T. Ramirez Reina, J. A. Odriozola, H. Arellano-Garcia), Wiley-VCH, Weinheim, **2021**, pp. 385–406.

[9] L. Guo, K. J. Lamb, M. North, *Green Chem.* **2021**, *23*, 77–118.

[10] A. J. Kamphuis, F. Picchioni, P. P. Pescarmona, *Green Chem.* **2019**, *21*, 406–448.

[11] N. Panza, A. di Biase, E. Gallo, A. Caselli, *J. CO_2 Util.* **2021**, *51*, 101635.

[12] C. Damiano, P. Sonzini, D. Intrieri, E. Gallo, *J. Porphyrins Phthalocyanines* **2020**, *24*, 809–816.

[13] J. K. Lamb, D. V. I. Ingram, M. North, M. Sengoden, *Curr. Green Chem.* **2019**, *6*, 32–43.

[14] A. Nazari, M. M. Heravi, V. Zadsirjan, *J. Organomet. Chem.* **2021**, *932*, 121629.

[15] Q. Zhao, L. Xin, Y. Liu, C. Liang, J. Li, Y. Jian, H. Li, Z. Shi, H. Liu, W. Cao, *J. Med. Chem.* **2021**, *64*, 10557–10580.

[16] J. M. Ready, *J. Med. Chem.* **2021**, *64*, 13212–13214.

[17] C. Foti, A. Piperno, A. Scala, O. Giuffrè, *Molecules* **2021**, *26*, 4280.

[18] T. Niemi, T. Repo, *Eur. J. Org. Chem.* **2019**, 1180–1188.

[19] M. Sengoden, M. North, A. C. Whitwood, *ChemSusChem* **2019**, *12*, 3296–3303.

[20] A. W. Miller, S. T. Nguyen, *Org. Lett.* **2004**, *6*, 2301–2304.

[21] W.-M. Ren, Y. Liu, X.-B. Lu, *J. Org. Chem.* **2014**, *79*, 9771–9777.

[22] Y. Liu, C. Chen, Y. L. Hu, *J. Porous Mater.* **2022**, *29*, 131–142.

[23] Y.-N. Li, Q.-N. Xu, L.-F. Wu, Y.-H. Guo, H. Yue, J. Zhou, C.-L. Ge, H.-R. Chang, *J. Environ. Chem. Eng.* **2021**, *9*, 105607.

[24] Y. Song, Q. Sun, B. Aguila, S. Ma, *Catal. Today* **2020**, *356*, 557–562.

[25] Y. Zhou, W. Zhang, L. Ma, Y. Zhou, J. Wang, *ACS Sustainable Chem. Eng.* **2019**, *7*, 9387–9398.

[26] G. Bresciani, M. Bortoluzzi, G. Pampaloni, F. Marchetti, *Org. Biomol. Chem.* **2021**, *19*, 4152–4161.

[27] Z.-Z. Yang, L.-N. He, J. Gao, A.-H. Liu, B. Yu, *Energy Environ. Sci.* **2012**, *5*, 6602–6639.

[28] Y. Zhao, B. Han, Z. Liu, *Acc. Chem. Res.* **2021**, *54*, 3172–3190.

[29] Z.-Z. Yang, L.-N. He, S.-Y. Peng, A.-H. Liu, *Green Chem.* **2010**, *12*, 1850–1854.

[30] V. B. Saptal, B. M. Bhanage, *ChemSusChem* **2016**, *9*, 1980–1985.

[31] R. Chawla, A. K. Singh, L. D. S. Yadav, *RSC Adv.* **2013**, *3*, 11385–11403.

[32] L. An-Hua, D. Ya-Li, Z. Hui, Z. Jin-Ju, L. Xiao-Bing, *ChemCatChem* **2018**, *10*, 2686–2692.

[33] M. Lv, P. Wang, D. Yuan, Y. Yao, *ChemCatChem* **2017**, *9*, 4451–4455.

[34] B. Xu, P. Wang, M. Lv, D. Yuan, Y. Yao, *ChemCatChem* **2016**, *8*, 2466–2471.

[35] Y. Lu, Z. Chang, S. Zhang, S. Wang, Q. Chen, L. Feng, Z. Sui, *J. Mater. Sci.* **2020**, *55*, 11856–11869.

[36] D. Intrieri, C. Damiano, P. Sonzini, E. Gallo, *J. Porphyrins Phthalocyanines* **2019**, *23*, 305–328.

[37] V. Saptal, D. B. Shinde, R. Banerjee, B. M. Bhanage, *Catal. Sci. Technol.* **2016**, *6*, 6152–6158.

[38] S. Kumar, M. Y. Wani, C. T. Arranja, J. d. A. e Silva, B. Avula, A. J. F. N. Sobral, *J. Mater. Chem. A* **2015**, *3*, 19615–19637.

[39] D. Carminati, E. Gallo, C. Damiano, A. Caselli, D. Intrieri, *Eur. J. Inorg. Chem.* **2018**, 5258–5262.

[40] P. Sonzini, C. Damiano, D. Intrieri, G. Manca, E. Gallo, *Adv. Synth. Catal.* **2020**, *362*, 2961–2969.

[41] C. Damiano, P. Sonzini, G. Manca, E. Gallo, *Eur. J. Org. Chem.* **2021**, 2807–2814.

[42] C. Damiano, P. Sonzini, M. Cavalleri, G. Manca, E. Gallo, *Inorg. Chim. Acta* **2022**, *540*, 121065.

[43] T. Nakanishi, K. Ohkubo, T. Kojima, S. Fukuzumi, *J. Am. Chem. Soc.* **2009**, *131*, 577–584.

[44] A. G. Mojarrad, S. Zakavi, *Catal. Sci. Technol.* **2018**, *8*, 768–781.

[45] P. Crotti, L. Favero, C. Gardelli, F. Macchia, M. Pineschi, *J. Org. Chem.* **1995**, *60*, 2514–2525.

[46] C. W. Kee, K. Q. E. Peh, M. W. Wong, *Chem. Asian J.* **2017**, *12*, 1780–1789.

[47] S. Grimme, *J. Chem. Phys.* **2006**, *124*, 034108.

[48] G. Norjmaa, G. Ujaque, A. Lledos, *Top. Catal.* **2022**, *65*, 118–140.

[49] J. R. Pliego, Jr., J. M. Riveros, *WIREs Comput. Mol. Sci.* **2020**, *10*, e1440.

[50] *Gaussian 16, Revision C.01*, M. J. Frisch, G. W. Trucks, H. B. Schlegel, G. E. Scuseria, M. A. Robb, J. R. Cheeseman, V. Barone, G. A. Petersson, H. Nakatsuji, X. Li, M. Caricato, A. V. Marenich, J. Bloino, B. G. Janesko, R. Gomperts, B. Mennucci, H. P. Hratchian, J. V. Ortiz, A. F. Izmaylov, J. L. Sonnenberg, D. Williams-Young, F. Ding, F. Lipparini, F. Egidi, J. Goings, B. Peng, A. Petrone, T. Henderson, D. Ranasinghe, V. G.

Chemistry–A European Journal

Research Article
doi.org/10.1002/chem.202202729

Chemistry Europe
European Chemical
Societies Publishing

Zakrzewski, J. Gao, N. Rega, G. Zheng, W. Liang, M. Hada, M. Ehara, K. Toyota, R. Fukuda, J. Hasegawa, M. Ishida, T. Nakajima, Y. Honda, O. Kitao, H. Nakai, T. Vreven, K. Throssell, J. A. Montgomery Jr., J. E. Peralta, F. Ogliaro, M. J. Bearpark, J. J. Heyd, E. N. Brothers, K. N. Kudin, V. N. Staroverov, T. A. Keith, R. Kobayashi, J. Normand, K. Raghavachari, A. P. Rendell, J. C. Burant, S. S. Iyengar, J. Tomasi, M. Cossi, J. M. Millam, M. Klene, C. Adamo, R. Cammi, J. W. Ochterski, R. L. Martin, K. Morokuma, O. Farkas, J. B. Foresman, and D. J. Fox, Gaussian, Inc., Wallingford CT, **2016**.

[51] V. Barone, M. Cossi, *J. Phys. Chem. A* **1998**, *102*, 1995–2001.
[52] M. Cossi, N. Rega, G. Scalmani, V. Barone, *J. Comput. Chem.* **2003**, *24*, 669–681.